

## Effects of Initial Energies on Mass Spectra\*

CLIFFORD E. BERRY

Consolidated Engineering Corporation, Pasadena, California

(Received January 16, 1950)

The slit system of a conventional mass spectrometer discriminates against ions having initial kinetic energies. Relations between the amount of the discrimination and the geometry of the system are developed and confirmed experimentally for ions having only thermal energy. Curves showing the discrimination against high energy fragments from a number of simple molecules are given. These curves show that measured relative abundances depend strongly on the geometry of the system and on the accelerating voltage.

In theory, the initial velocity distribution can be obtained from discrimination data. This method is shown to be impractical, and a better method is described, which involves electrostatic deflection of the ion beam in a direction parallel to the magnetic field. Curves of ion intensity *vs.* deflecting potential give directly the shape of the distribution for one component of initial velocity. Distribution curves are given for the same ions for which discrimination curves were obtained.

### 1. INTRODUCTION

CONVENTIONAL mass spectrometers exhibit a phenomenon called *discrimination*, in which ions having initial energies may fail to pass through the slit system of the ion source and analyzer tube because of the effects of the components of velocity normal to the principal motion through the system. It is found in general that ions having no initial kinetic energy except that due to thermal motions are discriminated against, even at accelerating voltages of several thousands of volts. In addition it is well known<sup>1</sup> that many molecules, when fragmented by electron impact, produce ions having as much as several volts excess kinetic energy. Such ions may be discriminated against to such an extent that very few are observed reaching the collector.

In the practical design and operation of mass spectrometers it is of interest to know what discrimination effects may take place, and to know their relation to the geometry of the system. This is particularly true of instruments used for isotope ratio measurements or for gas analysis. In addition, there is the possibility of utilizing the discrimination effect to determine average values of initial kinetic energies, and possibly to determine energy distributions, from which information regarding the potential energy curve for certain states of the molecule may be deduced.

The literature on the subject of discrimination itself is somewhat limited. Hagstrum and Tate,<sup>2</sup> in studying ionization processes, discussed qualitatively the discrimination against high energy ions at the first slit of a mass spectrometer. Coggeshall<sup>3</sup> was the first to show that even thermal velocities are great enough to cause measurable discrimination at the second slit of a conventional mass spectrometer, and that appreciable errors in isotope ratio measurement might result.

Washburn and Berry<sup>4</sup> pointed out that discrimination at the collector slit could be of the same order of magnitude as the discrimination at the second slit. They showed a set of discrimination curves for a number of ions from *n*-butane and attempted to estimate the initial energies of the various ions.

In work on molecular structure there have been numerous studies of the ionization process by electron impact, and while much of this work has been concerned with appearance potential measurements, some attention has been given to kinetic energy measurements, both in the mass spectrometer and in the retarding field apparatus of Lozier.<sup>5,6</sup> However, since Lozier's method cannot distinguish between ions of different mass-to-charge ratio, its use is somewhat limited.

Hagstrum and Tate<sup>2</sup> were able to make some deductions concerning the shape and position of the upper potential energy curves for a number of diatomic molecules by studying the peak shapes of the high energy ions in a mass spectrometer. Newhall<sup>7</sup> used the retarding

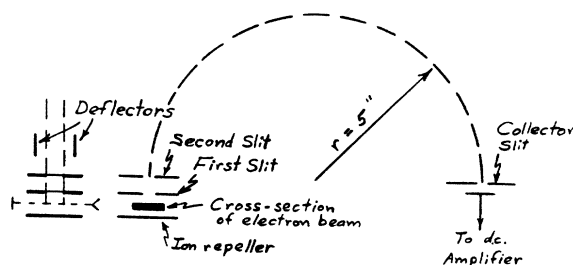


FIG. 1. Arrangement of slits in the mass spectrometer used in the experiments. For most of the discrimination experiments the dimensions were as follows: First slit,  $0.008 \times 0.250$  in.; second slit,  $0.008 \times 0.250$  in.; collector slit,  $0.030 \times 0.250$  in. The separation of the first and second slits was 0.250-in. For the deflection experiments, the lengths of the second slit and collector slit were changed from 0.250 to 0.040 in.

\* An abridgement of a thesis submitted to the Graduate Faculty of Iowa State College in partial fulfilment of the requirements for the degree of Doctor of Philosophy.

<sup>1</sup> E. E. Hanson, Phys. Rev. **51**, 86 (1937).

<sup>2</sup> H. D. Hagstrum and J. T. Tate, Phys. Rev. **59**, 354 (1941).

<sup>3</sup> N. D. Coggeshall, J. Chem. Phys. **12**, 19 (1944).

<sup>4</sup> H. W. Washburn and C. E. Berry, Phys. Rev. **70**, 559 (1946).

<sup>5</sup> W. W. Lozier, Phys. Rev. **36**, 1285 (1930).

<sup>6</sup> W. W. Lozier, Phys. Rev. **46**, 268 (1934).

<sup>7</sup> H. F. Newhall, Phys. Rev. **62**, 11 (1942).

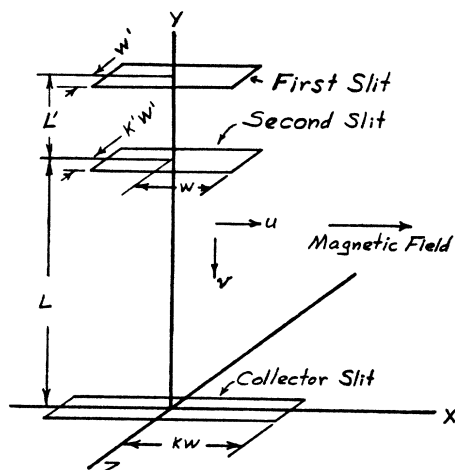


FIG. 2. Coordinate system used in deriving the discrimination equations for the collector slit and the second slit. The  $y$  axis has been shown straight for convenience; actually it is an arc of a circle.

potential produced by the space charge of the electron beam in a special mass spectrometer to study high energy protons. Hipple *et al.*<sup>8</sup> described the use of a retarding field near the collector in a mass spectrometer. Although their purpose was to suppress metastable ions, they demonstrated that the  $\text{CH}_3^+$  ion in *n*-butane may result from two processes, one giving ions of low initial energy and the other ions of high initial energy.

The problem which was undertaken in the present work was twofold: (a) To investigate theoretically and experimentally the effects of discrimination by the slits of a mass spectrometer, and (b) to explore methods of determining the distribution of initial velocities, in the hope of extending the usefulness of the mass spectrometer in the study of molecular structure.

## 2. THEORETICAL TREATMENT

### A. Derivation of Discrimination Equations

#### (a) Discrimination at the Collector Slit

Figure 1 shows the slit system of the mass spectrometer used in this study. The ions formed in the electron beam are forced through the first slit by a weak electric field, and are then accelerated in the region between the first and second slits by a voltage  $V$ . Between the second slit and the collector slit the ions travel at constant speed, but are caused to move in a circular path by the uniform magnetic field in which the entire apparatus is immersed. This is a conventional  $180^\circ$  mass spectrometer; the treatment that follows, however, applies to any mass spectrometer of the sector type, since the only geometrical factors concerned in the discrimination effect are the relative slit dimensions and spacings.

An approximate derivation of the discrimination at

the collector slit will be given first. Figure 2 shows the coordinate system and defines the pertinent quantities. It is assumed that ions pass through the second slit with a velocity  $v$  derived from the accelerating voltage, and in addition possess a small component of velocity  $\bar{u}$  at right angles to  $v$  in the direction of the plane of the slits.<sup>9</sup> We may consider  $\bar{u}$  to be the average molecular velocity corresponding to the temperature of the gas in the ionization region.

If we define collection efficiency  $N$  as the ratio of the number of ions of given mass passing through the collector slit in unit time to the number passing through the second slit, we can write from simple geometrical reasoning that

$$N = \begin{cases} 1 \\ k \end{cases} \quad \text{for } L\bar{u}/v < |k-1|w, \quad (1)$$

$$N = \frac{1}{2}(1+k - L\bar{u}/v) \quad \text{for } |k-1|w < L\bar{u}/v < (k+1)w, \quad (2)$$

$$N = 0 \quad \text{for } L\bar{u}/v > (1+k)w, \quad (3)$$

where the upper term in the bracket in Eq. (1) corresponds to  $k > 1$  and the lower to  $k < 1$ , and where  $k$  is the ratio of the length of the collector slit to the length of the second slit. Thus for either case, the collection efficiency is constant out to a critical value of  $L\bar{u}/v$  then, regarded as a function of  $L\bar{u}/v$ , decreases linearly to zero. If  $k=1$ , the initial flat portion of the curve disappears.

The relations just derived are applicable only when the spread in thermal velocities is small compared with  $v$ , so that the average value,  $\bar{u}$ , is representative. For

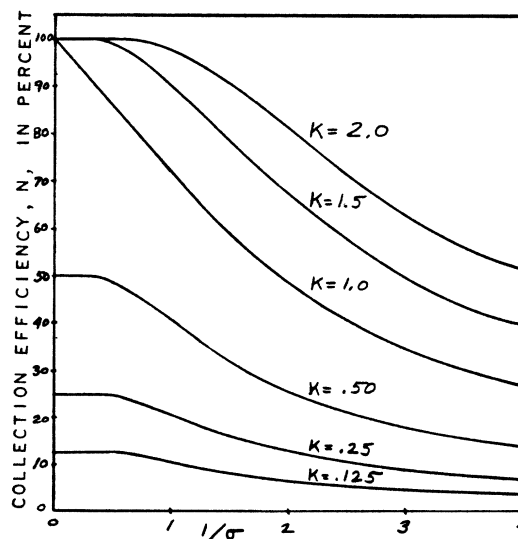


FIG. 3. Collection efficiency calculated from Eq. (4) in terms of the dimensionless parameter  $\sigma$ .

<sup>9</sup> Initial components in the  $y$  and  $z$  directions merely broaden the beam at the focal point, but since the beam is normally somewhat narrower than the collector slit, these components cause no loss of ions at the collector except at very low accelerating voltages.

<sup>8</sup> Hipple, Fox, and Condon, *Phys. Rev.* **69**, 347 (1946).

small values of  $v$ , the actual distribution of initial velocities must be considered. In the Appendix, the problem is solved for the general case of an arbitrary initial velocity distribution and also for a Maxwellian distribution. For the latter case, the result is found to be

$$N = \frac{1}{2}(k+1) \operatorname{erf}[(k+1)\sigma] - \frac{1}{2}|k-1| \operatorname{erf}[(k-1)\sigma] + (1/2\pi^{1/2}\sigma) [\exp[-(k+1)^2\sigma^2] - \exp[-(k-1)^2\sigma^2]], \quad (4)$$

in which  $\sigma$  is a dimensionless parameter defined as  $(108w/L)(V/T)^{1/2}$ ,  $V$  is the accelerating potential in volts, and  $T$  is the absolute temperature of the gas in degrees Kelvin. A plot of Eq. (4) for several values of the parameter,  $k$ , is shown in Fig. 3.

#### (b) Discrimination at the Second Slit

The discrimination effect at the second slit can be derived in a similar manner. Here the initial velocity component of interest is that at right angles to the plane of the slits. (Since the spacing of the first and second slits is normally nearly the same as the length of the slits, a velocity component parallel to the plane of the slits has relatively small effect.) The principal difference between this case and the previous one is that here the ions, instead of traversing the region with constant forward velocity, travel under constant acceleration. Thus the effects of initial velocity components are relatively twice as great. Equation (4) applies provided that  $\sigma$  is defined as  $(54w'/L')(V/T)^{1/2}$  and  $k'$  is substituted for  $k$ .

Coggeshall<sup>3</sup> derived an approximate expression for the discrimination effect at the second slit for the case  $k=1$ . If Eq. (4) is expanded in powers of  $\sigma$ , the first-order term is identical with Coggeshall's Eq. (16) when proper interpretation of symbols is made. Furthermore, the first-order approximation to Eq. (4) is identical with Eq. (2), the approximation derived previously.

Discrimination at the first slit can be treated in the same manner as that at the second slit if the thickness of the electron beam is assumed to be negligible. In the mass spectrometer used in the experimental work to be described, no discrimination at the first slit was observed because of the relatively great width of the electron beam as compared with the width of the first slit.

## B. Determination of Initial Energy Distributions

#### (a) Method Based on Discrimination Effect

Since the efficiency of collection,  $N$ , depends on the initial velocity distribution function  $\rho(u)$ , it should be possible, in theory at least, to find the distribution function from an experimental curve of  $N$  vs.  $V$ . If it is assumed that discrimination occurs only at the collector slit and that the value of the parameter  $k$  is unity, the problem is readily solved. The general expression for the collection efficiency (Eq. (9) in the Appendix)

in effect can be turned inside out to give an explicit expression for the initial *speed* distribution,  $F(s)$ , with the result

$$F(s) = -s^2 \frac{d^2 N(s)}{ds^3} - 3s \frac{d^2 N(s)}{ds^2}, \quad (5)$$

in which  $N(s)$  is the collection efficiency function.

For determining  $F(s)$  from an experimental curve for  $N$ , the use of Eq. (5) appears to be impracticable, since extremely smooth data would be required in order for the second and third differences to have meaning. Also,

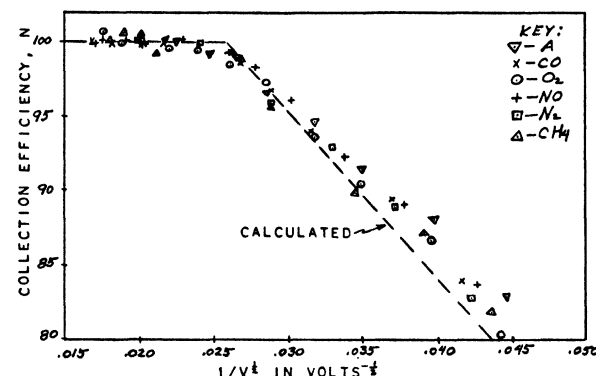


FIG. 4. Comparison of discrimination curves for a number of ions having only thermal energy. The calculated curve is based on the approximate treatment of Eqs. (1)–(3).

the problem would become much more complicated if  $k$  were different from unity or if discrimination at more than one slit occurred.

#### (b) Method Based on Deflection of Beam in Analyzing Region

A more promising method of determining initial velocity distributions is based on the use of a pair of small deflecting electrodes as shown in Fig. 1, placed immediately behind the entrance slit to the analyzing region so as to deflect the ion beam in the  $x$  direction. Such electrodes are used in some mass spectrometers in order to center the ion beam on the exit slit by compensating for mechanical misalignment.

As discussed earlier, the  $x$  component of initial velocity causes the beam to fan out in the  $x$  direction in the analyzing region. By making  $w/L$  sufficiently small, and thus the collection efficiency,  $N$ , likewise small, the collector slit in effect takes a small sample of the original beam, the sample consisting of those ions entering the analyzer with very small  $x$  components of velocity. By means of the deflecting electrodes, the fanned-out beam can be moved past the collector in the  $x$  direction, allowing each part of the original beam to be sampled.

It is easily shown that the curve of ion current vs. deflecting voltage gives directly the shape of the initial velocity curve for one component. The relation between the velocity scale and other pertinent factors is found

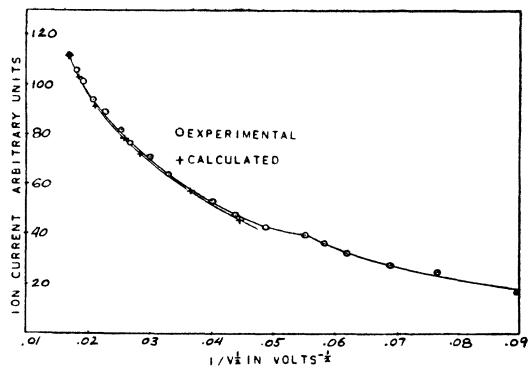


FIG. 5. Discrimination curve for  $\text{CO}^+$ , using 0.040-in. long second slit and collector slit. The calculated curve was obtained from Eq. (4).

to be

$$u = AP(e/mV)^{1/2}, \quad (6)$$

where  $A$  is a constant of the instrument,  $P$  the deflecting potential in volts,  $e$  the charge on the particle in e.s.u.,  $m$  the mass of the particle in grams, and  $V$  the accelerating potential in volts. In general the accurate calculation of the constant  $A$  is difficult. However, by calibrating the instrument with an ion of known velocity distribution and known energy, e.g., an ion with thermal energy,  $A$  can be determined empirically.

It is important to note in Eq. (6) that for an ion of given initial energy distribution, the experimental curve should be an invariant function of  $P/V^{1/2}$ , regardless of the constant value of  $V$  used. This is an excellent criterion for judging whether an instrument is measuring the true initial velocity distribution. If the collection efficiency is too high so that too broad a section of the distribution curve is sampled, then the distribution will appear different for different values of  $V$ , since the collection efficiency varies with  $V$ . Likewise, if end effects occur at the slits, the apparent distribution may be affected by the value of  $V$ , since some ions may receive  $x$  components of velocity from the accelerating field.

### 3. EXPERIMENTAL APPARATUS

The mass spectrometer used for the experimental work has been described in other publications.<sup>10-12</sup> The principal information needed in connection with the present work is that given in Fig. 1, which shows the slit dimensions and radius of curvature. The temperature of the ion source was 534°K, as determined by a thermocouple. It had been determined previously that the gas entering the ionizing region was in thermal equilibrium with the walls of the ion source.

The energy of the ionizing electrons was 100 volts for all experiments. The gas samples were approximately 99 percent or better in purity.

<sup>10</sup> C. E. Berry, *Electronic Industries* 3, 94 (June, 1944).

<sup>11</sup> Washburn, Wiley, Rock, and Berry, *Ind. Eng. Chem., Anal. Ed.* 17, 74 (1945).

<sup>12</sup> Washburn, Wiley, and Rock, *Ind. Eng. Chem., Anal. Ed.* 15, 541 (1943).

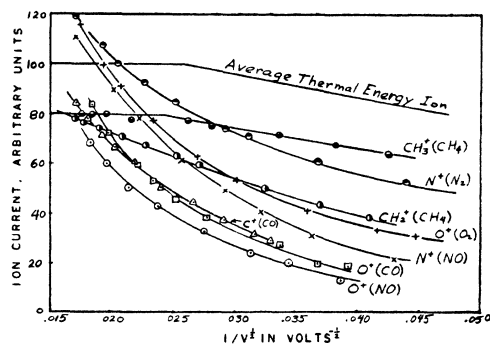


FIG. 6. Discrimination curves for the high energy fragments produced from a number of molecules. The discrimination curve for an average molecular ion is given for comparison. The scales are in arbitrary units, but the actual ratio of the current for a given fragment to the current for its parent molecule can be obtained by multiplying the scale for the fragment by the appropriate factor given:  $\text{C}^+$  from  $\text{CO}$  -0.059;  $\text{O}^+$  from  $\text{CO}$  -0.030;  $\text{O}^+$  from  $\text{O}_2$  -0.12;  $\text{N}^+$  from  $\text{N}_2$  -0.15;  $\text{O}^+$  from  $\text{NO}$  -0.047;  $\text{N}^+$  from  $\text{NO}$  -0.14;  $\text{CH}_2^+$  from  $\text{CH}_4$  -0.11;  $\text{CH}_2^{2+}$  from  $\text{CH}_4$  -1.1.

## 4. EXPERIMENTAL RESULTS

### A. Discrimination Experiments

#### (a) Ions with Thermal Energy

Equation (4), giving the collection efficiency for an ion with a Maxwellian distribution of initial velocities, reveals that the mass of the ion does not enter into the relation between collection efficiency and accelerating voltage. Thus, if no other effect than that postulated takes place, the curves of collection efficiency *vs.* accelerating voltage should be the same for all ions receiving no energy from dissociation processes.

Figure 4 compares the results of runs on the molecular ions formed in  $\text{CO}$ ,  $\text{A}$ ,  $\text{O}_2$ ,  $\text{N}_2$ ,  $\text{NO}$ , and  $\text{CH}_4$  which have only thermal energy. The points are seen to cluster very closely in a band two to three percent wide, thus confirming that primarily the discrimination effect, with only small extraneous effects, was taking place.

The abrupt change of slope observed in Fig. 4 was unexpected, inasmuch as previous work had shown no discrimination caused by the second ion slit. Furthermore, the nominal value of  $k$  for the collector slit was unity. However, the curves obtained are just what would be obtained from Eqs. (1) and (2) for  $k \neq 1$ . Since previous studies of deposits in the ion source had indicated that the ion beam was not perfectly collimated, the most reasonable explanation of the sharp break in the curves is that the beam of ions was either slightly diverging or slightly converging in the  $x$  direction (Fig. 2), so that effectively  $k$  differed from unity. A simple calculation shows that a half-angle of convergence in the  $x$  direction of  $0.25^\circ$  would give the calculated curve shown in Fig. 4 and would correspond to an effective value of 1.56 for  $k$ .

The discrimination curve for the molecular ion  $n\text{-C}_4\text{H}_{10}^+$  was found to contain a break, but the left-hand portion of the curve was not horizontal. Such an

effect could be caused by metastable ions, which are known to be formed in this molecule. Using Hipple's value<sup>13</sup> for the half life of the metastable  $n\text{-C}_4\text{H}_{10}^+$  ions, the experimental curve was corrected to give a curve closely matching those of Fig. 4. However, it was necessary to assume that 29 percent of the  $n\text{-C}_4\text{H}_{10}^+$  ions were originally in a metastable state, rather than 9 percent as Hipple estimated.

(b) *Discrimination at the Second Slit*

The results of all runs thus far described were completely explained by assuming that only the collector slit was active in discriminating against ions with thermal energy. This was considered reasonable in view of previous observations of deposits on the second slit. These observations indicated that because of lens action at the first slit, the beam striking the plane of the second slit was considerably wider than the slit itself. In this case there should be an effective value for  $k'$  somewhat less than unity.

In order to test this hypothesis, several runs were made, using the  $\text{CO}^+$  ion at much lower accelerating voltages (down to 60 volts) than were used previously. A second sharp break in the curve appeared at an accelerating voltage of about 340 volts, which is somewhat below the values commonly used in the normal operation of the mass spectrometer. From the position of this break, an effective value of 0.46 for  $k'$  was computed, which checks fairly well with measurements of deposits in the ion source.

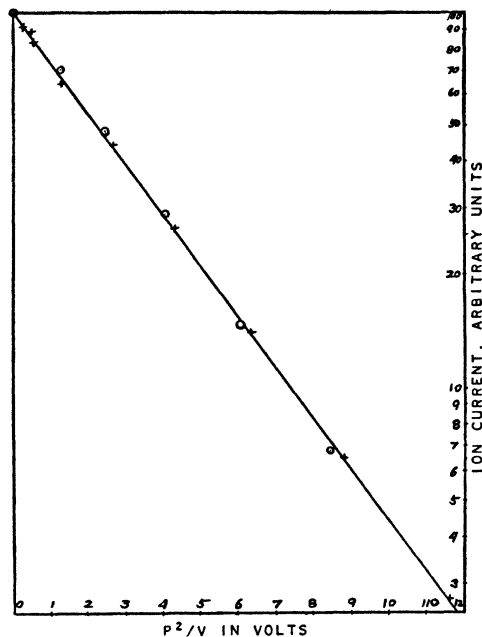


FIG. 7. Deflection experiment for  $\text{CO}^+$  ion. By plotting the log of the intensity vs. the square of the deflecting voltage, the curve should be linear if the distribution is Maxwellian.

<sup>13</sup> J. A. Hipple, Scientific Paper # 1264, Westinghouse Research Laboratories, East Pittsburgh, Pa. (1946).

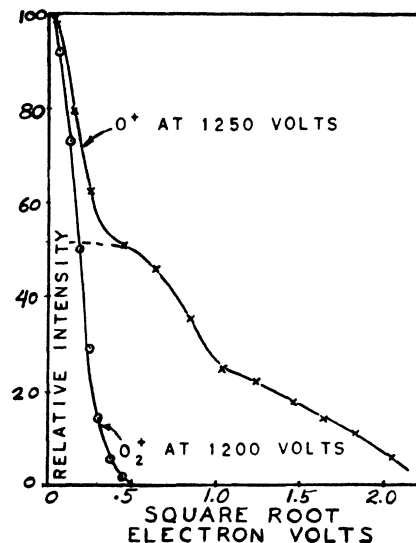


FIG. 8. Velocity distribution curves for  $\text{O}^+$  and  $\text{O}_2^+$  from  $\text{O}_2$ . The dotted line is an estimated distribution assuming the central hump to be  $\text{O}^{++}$  ions with thermal energy.

A further check on the discrimination effect for thermal energy ions was obtained by running  $\text{CO}^+$  with the entrance slit and collector slits cut down in length from 0.250 to 0.040 in. by means of apertured disks placed in the analyzer. The results of this run are shown in Fig. 5. The lower break, attributed to the second slit, did not change in position, but the upper one completely disappeared.

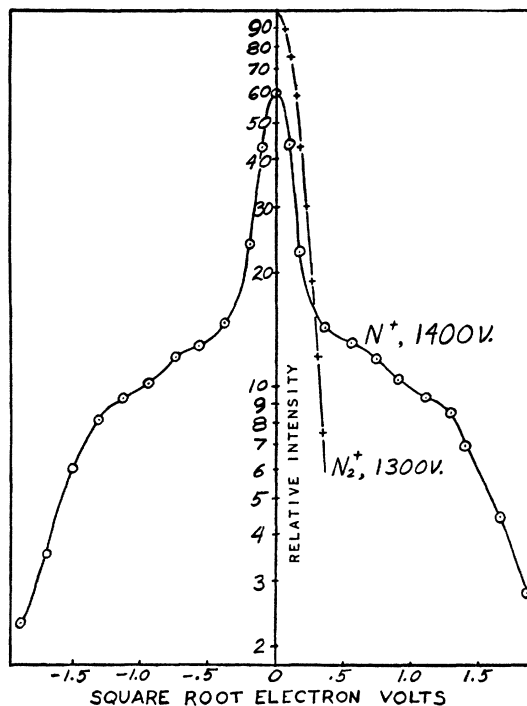


FIG. 9. Velocity distribution curves for  $\text{N}^+$  and  $\text{N}_2^+$  from  $\text{N}_2$ .

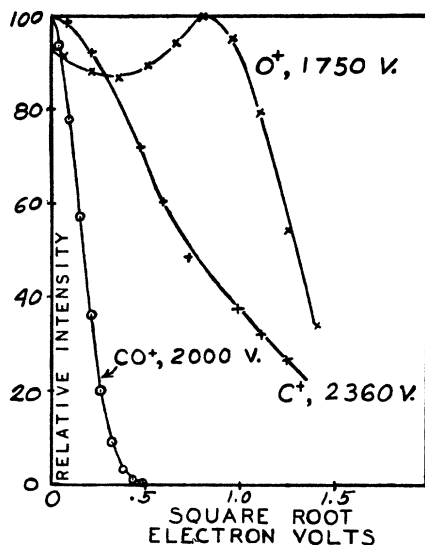


FIG. 10. Velocity distribution curves for  $C^+$ ,  $O^+$ , and  $CO^+$  from  $CO$ .

That portion of the curve to the left of the break, for which only the collector slit was responsible, afforded an excellent check on Eq. (4). The effective value of  $k$  was assumed to be unity, since only ions near the axis of the tube were collected. With this assumption, Eq. (4) for the collection efficiency was computed for the values of  $w$ ,  $L$ , and  $T$  used in the experiment. The theoretical points are shown as crosses in Fig. 5. The vertical scale factor was adjusted to fit at an arbitrarily chosen point; the agreement is seen to be good.

(c) *Discrimination Against High Energy Ions*

Figure 6 shows the result of discrimination runs on the high energy fragments resulting from ionization of  $CO$ ,  $O_2$ ,  $N_2$ ,  $NO$ , and  $CH_4$ . Plotted on the same sheet is the average curve for the thermal energy molecular ions. The scale factor for the molecular ions has been normalized, whereas the scale factors for the high energy ions are in arbitrary units. However, in each case a conversion factor is given by which the actual ion currents of the low and high energy ions can be related.

In general, the curves for the high energy ions are seen to be extremely steep when compared with that for thermal energy ions. It is probable that for the high energy ions shown, except the  $CH_3^+$  ion from methane, each curve is in the region below the second break; that is, in the region where both the collector slit and the second slit are discriminating.

The  $CH_3^+$  ion from methane appears to have but little excess energy, since the first break has moved only to a slightly higher voltage. Because of the scatter of points the position of the break for the  $CH_3^+$  curve is not definite. However, by comparing the slope of this curve with that of the  $CH_4^+$  curve, the average energy of the  $CH_3^+$  was found to be approximately 46 percent higher than thermal energy. This gives a value

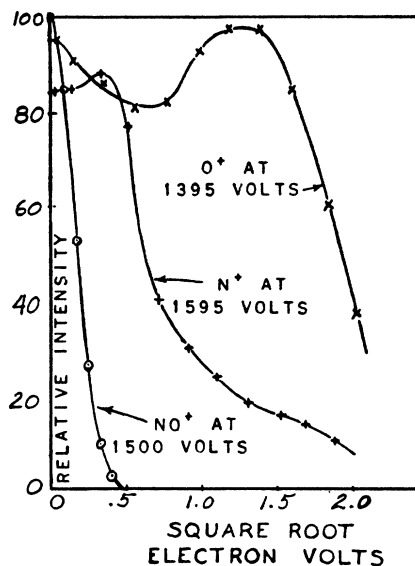


FIG. 11. Velocity distribution curves for  $N^+$ ,  $O^+$ , and  $NO^+$  from  $NO$ .

of 0.032 eV for the average excess kinetic energy of the  $CH_3^+$  ions.

It may be concluded that, insofar as the discrimination effect is concerned, the simple theory presented here adequately describes the effect. It is plain from a study of the curves given that the observed spectrum of a given substance will depend strongly on the geometry of the instrument used to obtain that spectrum.

The use of discrimination curves to estimate average initial energy appears to be valid for low energy ions. For high initial energies the method proposed becomes

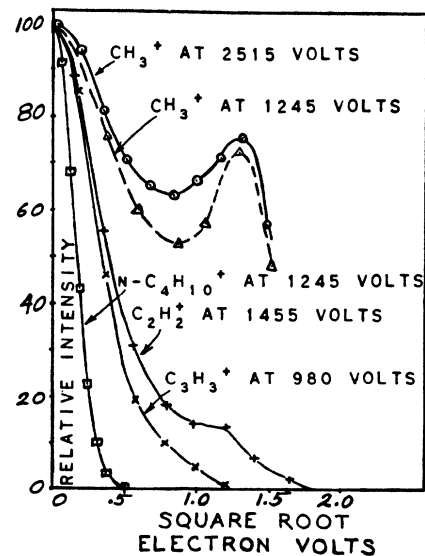


FIG. 12. Velocity distribution curves for various ions from  $n-C_4H_{10}$ . The dotted curve shows the effect of changing the accelerating voltage on the anomalous distribution for the  $CH_3^+$  ion.

too indirect to be of any use. In this connection it should be pointed out that the data presented by Washburn and Berry,<sup>4</sup> on the average initial energies of some ions from *n*-butane, were based on imperfect knowledge of the effects of discrimination and the influence of the energy distributions on the slopes of the curves, and the figures given can only be rough approximations.

## B. Deflection Experiments

### (a) Test of the Method

The principal test of the deflection method was to see whether the measured distribution curve for an ion having a Maxwellian distribution gave the correct curve experimentally. Figure 7 shows a typical result on an ion with thermal energy, the  $\text{CO}^+$  ion. For a Maxwellian distribution, plotting the log of the intensity against the velocity squared should give a straight line. The curve shown was drawn through the experimental points with a straightedge by estimating the best average position. The good linearity over a range of intensity of nearly 40 to 1 shows a close agreement with Maxwell's distribution law and gives confidence in the method.

Further tests, using ions of different masses, and the same ion at different accelerating voltages, gave reasonably consistent results. Runs of this sort were used to establish the energy scales for the distribution curves of the high energy ions.

### (b) Distributions for High Energy Ions

Figures 8 through 12 show the results of runs on the high energy ions observed in  $\text{O}_2$ ,  $\text{N}_2$ ,  $\text{CO}$ ,  $\text{NO}$ , and *n*- $\text{C}_4\text{H}_{10}$ , respectively. Plotted on each sheet are also the distributions for the respective molecular ions. Each curve gives the shape of the distribution for one component of velocity, plotted in square root electron volts so that energy distributions can be calculated readily.

#### $\text{O}^+$ from $\text{O}_2$

The distribution curve of Fig. 8 shows the probable presence of three groups of ions, one having essentially thermal energy (probably  $\text{O}_2^{++}$  ions) one having a minimum energy of about 0.17 ev, and one having a minimum energy of about 1.1 ev. These latter groups correspond to transitions giving rise to the "Type II" peak shapes of Hagstrum and Tate.<sup>2</sup>

#### $\text{N}^+$ from $\text{N}_2$

The curve of Fig. 9 is similar to the curve for  $\text{O}^+$  from  $\text{O}_2$ , showing again three distinct groups of ions, one having essentially thermal energy, one having a minimum energy at about 0.5 ev, and the third having a minimum energy of about 1.9 ev.

#### $\text{C}^+$ and $\text{O}^+$ from $\text{CO}$

The  $\text{C}^+$  ion shows a smooth curve (Fig. 10) rising to a maximum at zero with no abrupt changes in slope,

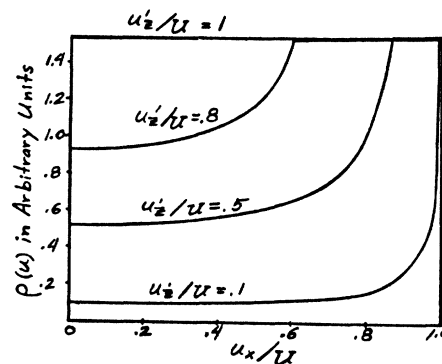


FIG. 13. Theoretical distribution functions, showing the distortion produced by discrimination.

indicating that many ions are formed with energies near zero. This is in general agreement with the results of Hagstrum and Tate for this particular ion.

The result for the  $\text{O}^+$  ion from  $\text{CO}$  is anomalous in that a minimum occurs at zero velocity. In any physical situation where spherical symmetry obtains, the distribution of one component of velocity cannot have a positive slope at any point, as this implies a negative value for a portion of the speed distribution function. Neglecting this for the moment, it is apparent that very few, if any ions of less than about 0.65 ev are formed, and that appreciable numbers are formed with more than 2.5 ev. This also is in general agreement with the result of Hagstrum and Tate on  $\text{CO}$ .

#### $\text{N}^+$ and $\text{O}^+$ from $\text{NO}$

Both curves of Fig. 11 for  $\text{NO}$  show the same anomaly as observed with the  $\text{O}^+$  ion from  $\text{CO}$ . As the ion currents for the  $\text{O}^+$  and  $\text{N}^+$  peaks were rather weak, the scatter of points is somewhat worse than for some of the other gases. However, there is a definite dip in each distribution. In the case of the  $\text{N}^+$  ion, there appear to be no ions formed with less than 0.1 ev, while for the  $\text{O}^+$  ion, all appear to have at least 2 ev. This result for  $\text{O}^+$  disagrees with that of Hagstrum and Tate, since they suggest that appreciable numbers of  $\text{O}^+$  ions are formed with zero energy. They give no result for the  $\text{N}^+$  ion.

#### $\text{CH}_3^+$ , $\text{C}_2\text{H}_2^+$ , $\text{C}_3\text{H}_3^+$ from *n*- $\text{C}_4\text{H}_{10}$

The curves of Fig. 12 for the  $\text{C}_2\text{H}_2^+$  ion and the  $\text{C}_3\text{H}_3^+$  ion show that ions of several volts energy are produced, but that many low energy ions are also produced. Since it is probable that many different types of processes can give rise to these ions, the curves are undoubtedly the superposition of several different distributions.

The distribution curve for the  $\text{CH}_3^+$  ion is more interesting. Here again the same anomaly is observed as with some of the previous ions. However, there is a rise in the center, suggesting the presence of a group of  $\text{CH}_3^+$  ions with low, perhaps only thermal, energies. This is in agreement with the results of Hipple,<sup>8</sup> who

found evidence for the existence of a high energy group and a low energy group for this ion.

The most likely reason for the anomalous curves obtained for  $N^+$  and  $O^+$  from NO,  $O^+$  from CO, and  $CH_3^+$  from  $n-C_4H_{10}$  becomes apparent when the effects of discrimination at the second slit are considered. It has been tacitly assumed thus far that the ions emerging from the second slit have a spherically symmetrical distribution of initial velocities. However, if any component is discriminated against the distribution of every other component is changed. In the present instance it is known that the second slit discriminated against ions with high initial velocities in the  $z$  direction. Thus it should be expected that the  $x$  component of velocity, which is the component affected by the deflecting potential, would suffer a distortion of its distribution function.

The effect, on the  $x$  velocity distribution, of losing all ions with  $z$  components of velocity above a certain amount is readily calculated. Figure 13 summarizes the results. It is assumed that all ions have initially the same velocity  $U$ , uniformly distributed in direction, and that those ions with  $z$  components of velocity greater than  $u_z'$  are lost. The curves show the distribution in  $x$  components of velocity for  $u_z'/U=0.1, 0.5, 0.8,$  and  $1.0$ . It is seen that the distributions have minima at zero velocity and reach a maximum at a point dependent upon  $u_z'/U$ . Beyond this point the distribution is uniform out to  $u_x/U=1$ .

In any actual case, the distribution of initial velocities would have a spread of values, so that a superposition of distributions such as those shown in Fig. 13 would occur. However, if there were a minimum value of the initial speeds the superposition would then result in a velocity distribution curve with a minimum at zero velocity, such as that found for  $O^+$  from CO, for example. On the other hand, if large numbers of ions with both low and high velocities were formed the over-all distribution of one component of velocity, while distorted by the discrimination effect, still would not necessarily show a dip in the center.

The effect just mentioned should become greater the lower the accelerating voltage. This is borne out by the dotted curve of Fig. 12, which shows the distribution for the  $CH_3^+$  ion from  $n-C_4H_{10}$  at 1245 volts. The solid curve, taken at 2515 volts, shows the same general shape but has a less pronounced dip.

It is clear that precise use of the deflection method in the present apparatus is limited to those ions with such low energies that discrimination at the second slit does not occur. Consideration of the discrimination curves for the second slit indicates that, at an accelerating voltage of about 2000 volts, negligible second slit discrimination would occur against those ions which had their principal energies below about six times thermal energy. In order to obtain accurate distribution curves for higher energy ions a modification of the ion

source would have to be made to reduce the second slit discrimination.

The direction in which to proceed to reduce the second slit discrimination is indicated by Eq. (1). By increasing the width of the first slit, and making  $k'$  smaller (assuming it to be less than unity originally), the maximum value of the initial velocity that will be free of discrimination can be increased. For example, increasing the first slit width by a factor of three and decreasing the second slit width by a factor of two should result in an increase of a factor of 5.5 in the maximum initial velocity that would be discrimination free. This corresponds to a 30-fold increase in the initial energy. Reference to the velocity distribution curves shown in Figs. 8-12 shows that such a modification should allow much more accurate distribution curves to be obtained.

Despite the fact that the velocity distributions shown are distorted from the true distributions, they are of interest in indicating the magnitudes of the initial dissociation energies of the molecules studied. Furthermore, the sharp breaks occurring in some of the curves undoubtedly indicate the presence of certain transitions taking place within the molecules.

The writer wishes to express his gratitude to Dr. H. W. Washburn for many suggestions during the course of the work, to Dr. Sam Legvold for his encouragement and suggestions regarding the manuscript, and to Consolidated Engineering Corporation for the use of the mass spectrometer and for permission to publish this work.

## APPENDIX

Derivation of the discrimination equation for an arbitrary initial velocity distribution and for a Maxwellian distribution.

For an arbitrary distribution of velocities,  $\rho(u)$ , Eqs. (1) and (2) can be rewritten as

$$dN_u = \left\{ \frac{1}{k} \right\} \rho(u) du \quad \text{for } Lu/v < |k-1|w, \quad (7)$$

$$dN_u = \frac{1}{2}(1+k-Lu/vw)\rho(u)du \quad \text{for } |k-1|w < (Lu/v) < (k+1)w. \quad (8)$$

Integrating (7) and (8) between the limits indicated, and adding, there results for the over-all collection efficiency

$$N = 2 \left\{ \frac{1}{k} \right\} \int_0^{|k-1|wv/L} \rho(u) du + 2 \int_{|k-1|wv/L}^{(k+1)wv/L} \frac{1}{2}(1+k-Lu/vw)\rho(u) du, \quad (9)$$

where the factor 2 appears because only positive velocities are considered in the limits.

Now if the distribution of velocities is Maxwellian the indicated integrations can be carried out. The distribution of one component of velocity is given by

$$\rho(u) = (hm/\pi)^{1/2} \exp(-hmu^2), \quad (10)$$

where  $m$  is the mass of the particle in grams, and  $h=1/2RT$ , in which  $R$  is Boltzmann's constant in ergs/deg. C/molecule, and  $T$  is degrees Kelvin. Making this substitution, and setting



$\sigma = (w/L)(hm)^{\frac{1}{2}}$ , the final expression for  $N$  becomes

$$N = \frac{1}{2}(k+1) \operatorname{erf}[(k+1)\sigma] - \frac{1}{2}|k-1| \operatorname{erf}[(k-1)\sigma] + (1/2\pi^{\frac{1}{2}}\sigma)[\exp[-(k-1)^2\sigma^2] - \exp[-(k+1)^2\sigma^2]]. \quad (11)$$

This is a simple result, since all possible conditions are encompassed by the two dimensionless parameters  $k$  and  $\sigma$ . The parameter  $k$  is simply the ratio of the collector slit length to the entrance slit length;  $\sigma$  can be expressed in other terms, by substituting for  $k$  its equivalent expression given above, and for  $v$  in terms of the mass and charge of the particle and the accelerating voltage. When this is done, we obtain

$$\sigma = (w/L)(eV/300RT)^{\frac{1}{2}}. \quad (12)$$

Substitution of numerical factors for  $e$  and  $R$  gives

$$\sigma = 108w/L(V/T)^{\frac{1}{2}}.$$

The general discrimination equation, Eq. (9), for the special case of  $k=1$ , can be inverted to give an explicit expression for the initial speed distribution  $F(s)$  in terms of the collection efficiency function  $N(s)$ . Though tedious, the process simply involves repeated differentiation of the integrals of Eq. (9), and suitable rearrangement. The final result is

$$F(s) = -s^2 \frac{d^3 N(s)}{ds^3} - 3s \frac{d^2 N(s)}{ds^2}. \quad (13)$$

## On the Statistics of Luminescent Counter Systems\*

FREDERICK SEITZ

*University of Illinois, Urbana, Illinois*

AND

D. W. MUELLER

*Los Alamos Scientific Laboratory, University of California, Los Alamos, New Mexico*

(Received February 10, 1950)

The method of generating functions is employed to analyze the composite statistical variations which arise in a counting system that consists of a source, a luminescent crystal, and a photo-multiplier tube. The methods are applied to several photo-type assemblies and indicate that the techniques can be used to treat any problem of this type in a simple way. It is found that once the crystal has accepted energy, the effectiveness of the assembly is measured by the number of photo-electrons ejected from the photo-cathode of the multiplier. This quantity, which depends upon the luminescent efficiency of the crystal, the geometry of the crystal-multiplier arrangement and the efficiency of the photo-cathode, should be at least 5 for faithful counting of particles absorbed in the crystal. The number of photoelectrons must be much larger than 5 for good statistics if the current from the multiplier is measured. The results of Schiff and Evans for the statistical variations in the voltage of a condenser which is charged with the pulses from the multiplier are generalized to cover the case in which the size of pulses varies.

### 1. INTRODUCTION

THE type of crystal counter which depends upon the combination of luminescent crystals and a photo-multiplier tube shows promise of being of great service in the detection of radiations both because of its high sensitivity and its speed of registry and recovery. This device has been developed by a large number of individuals, almost too numerous to mention; however, the origin of the system appears to rest with Coltman and Marshall,<sup>1</sup> who employed powdered luminescent materials of the type used in previous commercial luminescent systems, and with Broser and Kallmann,<sup>2</sup> who first appreciated the advantages of employing large transparent luminescent crystals and introduced organic materials.

The purpose of the present paper is to analyze some

of the factors which influence the statistical behavior of luminescent counter systems in order to evaluate the limits within which a counter may be used in making a particular type of measurement. The problems of interest range over a wide spectrum of possibilities. However, the problem on which we shall focus attention for immediate purposes in order to provide a practical objective is the following: A crystal counter system is employed to count the gamma-rays emitted from a source in time  $T$ . If  $N$  gamma-rays are emitted, what is the most probable number that will be counted and what is the range of variation to be expected? We shall attempt to examine this problem in a sufficiently general way that the results will have value for a much broader group of problems.

It is interesting to consider the component parts of this problem in order to be able to examine the sources of statistical variations. The components are as follows.

(A) The source, even if constant in the sense that it remains unchanged during the time  $T$  will contribute to the statistical variation since the gamma-rays are usually emitted at random. For simplicity, we shall assume that the time  $T$  is sufficiently short that varia-

\* This document is based on work performed at Los Alamos Scientific Laboratory of the University of California under U. S. Government contract W-7405-Eng-36.

<sup>1</sup> J. W. Coltman and F. Marshall, *Phys. Rev.* **72**, 528 (1947); F. Marshall, *J. App. Phys.* **18**, 512 (1947).

<sup>2</sup> I. Broser and H. Kallmann, *Zeits. f. Naturforschung* **2a**, 439 (1937); 642 (1947); Broser, Herforth, Kallmann, and Martius, *Zeits. f. Naturforschung* **3a**, 6 (1948).